COBEM 2021 26th International Congress of Mechanical Engineering
November 22-26, 2021, Virtual Congress, Brazil
ABCM Associação Brasileira de Engenharia e Ciências Mecânicas

COB-2021-0097
IMPACT OF NON-NORMALITY IN LOCAL STABILITY ANALYSES OF POISEUILLE-RAYLEIGH-BÉNARD FLOWS

Gabriel Y. R. Hamada
William R. Wolf
School of Mechanical Engineering, University of Campinas, Campinas, SP, 13083-970, Brazil
gyrhamada@gmail.com, wolf@fem.unicamp.com
Diogo B. Pitz
Department of Mechanical Engineering, Federal University of Paraná, Curitiba, PR, Brazil
diogo.pitz@ufpr.br

Abstract. *This work presents a temporal local stability analysis of a Poiseuille-Rayleigh-Bénard (PRB) flow, which is important in several industrial applications such as chemical vapor deposition studies and cooling of electronic equipment. The linearized Navier-Stokes equations are solved assuming the Oberbeck-Boussinesq approximation. The wall-normal derivatives appearing in the linearized equations are discretized using a fourth-order finite difference scheme, while a Fourier mode decomposition is used in the streamwise and spanwise directions. Then, the resulting system is solved by a generalized eigenvalue problem. Initially, the modal approach is used to understand the flow stability properties in an infinite time horizon, i.e., following the definition of Lyapunov through analysis of the eigenvalue spectra. Since the modal analysis cannot provide insights of the non-normal properties of the flow, a non-modal approach is also considered. To employ this analysis, it is first necessary to establish an energy norm of the linear operator and, then, rewrite it into the matrix exponential form, which is solved by a singular value decomposition (SVD). Transient growth, resolvent and input-output analyses are employed to understand the flow behavior in a finite time. Results demonstrate that the increase of the non-dimensional parameters such as Reynolds and Rayleigh numbers enhance the effects of energy growth in both transient growth and input-output analyses.*

Keywords: *Poiseuille-Rayleigh-Bénard, input-output analysis, linear hydrodynamic stability, resolvent analysis*

1. INTRODUCTION

The Poiseuille-Rayleigh-Bénard (PRB) flow consists of a plane Poiseuille flow in the presence of an unstable temperature gradient imposed at the channel walls. Studies of PRB flows find applications in heat exchangers, electroplating, geophysical flows, electronics cooling, chemical vapor decomposition, among others. The first experimental studies of these flows were performed in the 1920s (Idrac, 1920) and were mainly concerned with applications in meteorology. More recently, Nicolas *et al.* (2000) investigated the influence of several physical parameters which play an important role in hydrodynamic stability of PRB flows, such as the Reynolds, Rayleigh and Prandtl numbers. These authors conducted a thorough analysis for a wide range of transversal aspect ratios in the channel by performing a bi-global modal analysis of the linearized system of Navier-Stokes equations including the Boussinesq approximation. They concluded that, even considering wall confinement, the Reynolds number for which the flow transitioned was higher than that observed in experimental studies. These results are important to show the limitations of the modal linear analysis. For a complete bibliographical review of the studies developed for PRB flows, we refer to the work by Nicolas (2002).

For plane Poiseuille flows, several non-modal techniques of stability analysis have been applied to provide further insights into the physical behavior of the flow, such as the transient growth of instabilities (Reddy and Henningson, 1993). In this case, the resolvent technique and an analysis of the system pseudospectrum can provide information in terms of non-normality of the eigenvectors that arise due to shear effects in the flow (Trefethen *et al.*, 1993). These effects may lead to transient growth of disturbances even in a stable fluid system (in an infinite time sense). When non-normality occurs, the amplification of disturbances in a finite-time horizon may trigger the growth of secondary instabilities and transition. This type of approach fits into a non-modal stability analysis framework as discussed by Schmid and Brandt (2014) and, through the application of an input-output analysis (Jovanović and Bamieh, 2005) it is possible to understand the flow response to input disturbances. For PRB flows, Sameen and Govindarajan (2007) and John Soundar Jerome *et al.* (2012) used the transient growth analysis to show that the unstable thermal stratification increases the maximum transient growth compared to pure shear flows. It was also noticed by these authors that the spanwise-uniform disturbances are not dominant in PRB flows at any condition, i.e., longitudinal disturbances are often more impactful in terms of transient growth magnitude.

The objective of this work is to investigate PRB flows with respect to their stability properties. For this, we perform a temporal local stability analysis of the linearized Navier-Stokes equations assuming the Oberbeck-Boussinesq approximation. Initially the modal approach is used to understand the flow stability properties in an infinite time horizon, i.e., following the definition of Lyapunov through analysis of the eigenvalue spectra. Results are compared to those from a Poiseuille flow in terms of the eigenvalues for validation of the code. Since the modal analysis cannot provide insights of the non-normal properties of the flow, a non-modal approach is also applied and results are presented in terms of transient growth of disturbances. A comparison is provided against the solutions from John Soundar Jerome *et al.* (2012) and excellent agreement is observed. Finally, an input-output analysis is performed to understand the response characteristics of the fluid system with respect to velocity and thermal forced disturbances

2. THEORETICAL FORMULATION

This section presents the theoretical methodology employed in this work for the study of hydrodynamic instabilities in a PRB flow. Linear analysis is employed using both modal and non-modal approaches. In the latter case, the resolvent formalism is also discussed to provide an input-output analysis of linear disturbances.

2.1 Governing equations

The governing equations that model the disturbances in PRB flows are obtained by linearizing the Navier-Stokes equations including the Oberbeck-Boussinesq approximation (see Chandrasekhar (1961)). The equations are linearized with respect to a base flow which is an equilibrium state of the dynamical system. Following the non-dimensionalization suggested by John Soundar Jerome *et al.* (2012), the equations can be written as

$$\begin{aligned}
&\frac{\partial u}{\partial x}+\frac{\partial v}{\partial y}+\frac{\partial w}{\partial z}=0\,,\\
&\frac{\partial u}{\partial t}+Re\,Pr\,U\frac{\partial u}{\partial x}+Re\,Pr\,w\frac{\partial U}{\partial z}=-\frac{\partial p}{\partial x}+Pr\nabla^2 u\,,\\
&\frac{\partial v}{\partial t}+Re\,Pr\,U\frac{\partial v}{\partial x}=-\frac{\partial p}{\partial y}+Pr\nabla^2 v\,,\\
&\frac{\partial w}{\partial t}+Re\,Pr\,U\frac{\partial w}{\partial x}=-\frac{\partial p}{\partial z}-\frac{Ra\,Pr}{16}\theta+Pr\nabla^2 w\,,\text{ and}\\
&\frac{\partial \theta}{\partial t}+Re\,Pr\,U\frac{\partial \theta}{\partial x}+w\frac{\partial \Theta}{\partial z}=\nabla^2\theta\,.
\end{aligned}\tag{1}$$

The parameters appearing in the equations above are the Reynolds number, $Re = U_{max}(H/2)/\nu$, the Prandtl number, $Pr = \nu/\alpha$, and the Rayleigh number, $Ra = g\beta\Delta T H^3/(\nu\alpha)$. In these parameters, g is the gravitational acceleration, β is the thermal expansion coefficient, ν is the kinematic viscosity, α is the thermal diffusivity, H is the channel height, and U_{max} is the maximum velocity. The terms (u, v, w), θ and p represent the perturbation velocities, temperature and pressure, respectively, and ΔT is the temperature difference between the channel walls.

The normalized velocity and temperature profiles for the PRB flow are given by

$$U(z) = 1 - z^2, \quad \text{and} \quad \Theta(z) = -z. \tag{2}$$

The flow domain is assumed to be infinite in the streamwise (x) and spanwise (y) directions, allowing the application of a Fourier transform in both cases as

$$\mathbf{q}(x, y, z, t) = \hat{\mathbf{q}}(z, t)\exp\{i(kx + my)\}, \quad \text{where} \quad \mathbf{q} = (u, v, w, \theta, p)^T\,. \tag{3}$$

The coefficients k and m represent the streamwise and spanwise wavenumbers, respectively. By applying Eq. (3) into Eq. (1), the governing equations are simplified to

$$\begin{aligned}
&ik\hat{u}+im\hat{v}+D\hat{w}=0\,,\\
&\frac{\partial \hat{u}}{\partial t}+Re\,Pr\,U\,ik\hat{u}+Re\,Pr\,\hat{w}DU=-ik\hat{p}+Pr[-\hat{u}(k^2+m^2)+D^2\hat{u}]\,,\\
&\frac{\partial \hat{v}}{\partial t}+Re\,Pr\,U\,ik\hat{v}=-im\hat{p}+Pr[-\hat{v}(k^2+m^2)+D^2\hat{v}]\,,\\
&\frac{\partial \hat{w}}{\partial t}+Re\,Pr\,U\,ik\hat{w}=-D\hat{p}+\frac{Ra\,Pr}{16}\hat{\theta}+Pr[-\hat{w}(k^2+m^2)+D^2\hat{w}]\,,\text{ and}\\
&\frac{\partial \hat{\theta}}{\partial t}+Re\,Pr\,U\,ik\hat{\theta}+\hat{w}D\Theta=[-\hat{\theta}(k^2+m^2)+D^2\hat{\theta}]\,,
\end{aligned}\tag{4}$$

where $D = \partial/\partial z$ is discretized using a fourth-order finite difference scheme. The boundary conditions are applied as $\hat{\mathbf{q}}(z = \pm 1) = 0$ and Eq. (4) can be represented as a linear system as

$$\mathbf{R}\frac{\partial}{\partial t}\hat{\mathbf{q}} = \mathbf{L}\hat{\mathbf{q}}\,, \tag{5}$$

where

$$\mathbf{R} = \begin{bmatrix} 1 & 0 & 0 & 0 & 0 \\ 0 & 1 & 0 & 0 & 0 \\ 0 & 0 & 1 & 0 & 0 \\ 0 & 0 & 0 & 1 & 0 \\ 0 & 0 & 0 & 0 & 0 \end{bmatrix}, \quad \mathbf{L} = \begin{bmatrix} -L_1 & 0 & -RePrDU & 0 & -ik \\ 0 & -L_1 & 0 & 0 & -im \\ 0 & 0 & -L_1 & RaPr/16 & -D \\ 0 & 0 & -D\Theta & -L_2 & 0 \\ -ik & -im & -D & 0 & 0 \end{bmatrix}. \tag{6}$$

In the previous linear equation, the operators L_1 and L_2 are written as $L_1 = ik\,Re\,Pr\,U + Pr[k^2 + m^2 - D^2]$ and $L_2 = ik\,Re\,Pr\,U + [k^2 + m^2 - D^2]$.

2.2 Modal analysis

Since $\mathbf{R}$ is a singular matrix, the solution of Eq. (5) is obtained by the generalized eigenvalue problem for $\mathbf{R}$ and $\mathbf{L}$. Hence, the linear system is rewritten as

$$\frac{\partial}{\partial t}\hat{\mathbf{q}} = \tilde{\mathbf{L}}\hat{\mathbf{q}}; \quad \text{with } \tilde{\mathbf{L}} = \mathbf{V}\mathbf{\Lambda}\mathbf{V}^{-\mathbf{1}}\,, \tag{7}$$

where $\mathbf{\Lambda}$ and $\mathbf{V}$ are the eigenvalue and eigenvector matrices, respectively. For the modal analysis, a Laplace transform is applied for the temporal dynamics since the stability of the fluid system is evaluated in an infinite time horizon. This allows the analysis of separate frequencies as

$$\hat{\mathbf{q}}(z,t) = \tilde{\mathbf{q}}(z)\exp\left(-i\omega t\right). \tag{8}$$

Substitution of Eq. (8) into Eq. (7) results in the following eigenvalue problem

$$-i\omega\tilde{\mathbf{q}} = \tilde{\mathbf{L}}\tilde{\mathbf{q}}\,. \tag{9}$$

Setting real values for the wavenumbers (k, m) and solving Eq. (9) yields the eigen spectrum. By evaluating the spectrum it is possible to state whether the base flow is linearly stable or unstable with respect to infinitesimal disturbances at particular frequencies.

2.3 Non-modal analysis

For non-modal analysis, Eq. (7) is rewritten as

$$\hat{\mathbf{q}}(t) = \exp\left(t\tilde{\mathbf{L}}\right)\hat{\mathbf{q}}_0\,. \tag{10}$$

In this case, non-normality of the eigenvectors due to shear effects is taken into account and the dynamical system may exhibit transient growth for a finite time horizon even if its energy decays at $t \to \infty$. This transient growth is defined as

$$G(t) = \max_{\mathbf{q}_0}\frac{E(\hat{\mathbf{q}}(t))}{E(\hat{\mathbf{q}}_0)} = ||\exp\left(t\tilde{\mathbf{L}}\right)||_E^2\,, \tag{11}$$

where E refers to an energy norm. For this work, the energy norm is defined using the form established by John Soundar Jerome *et al.* (2012), which includes both the kinetic and thermal energies of disturbances as

$$E(t) = \int_{-1}^{1}\frac{1}{2}\left[|\hat{u}|^2 + |\hat{v}|^2 + |\hat{w}|^2 + RaPr|\hat{\theta}|^2\right]dz\,. \tag{12}$$

The energy norm can be applied directly into $\tilde{\mathbf{L}}$ by the following transformation

$$\tilde{\mathbf{L}}_E = (\mathbf{EV})\mathbf{\Lambda}(\mathbf{EV})^{-1}\,, \tag{13}$$

where $\mathbf{E} = \text{diag}(1,1,1,\sqrt{RaPr},0)/\sqrt{2}$. The transient growth calculation from Eq. (11) can be obtained by applying the SVD at each time step and storing the first singular value, which represents the energy of the perturbation at that time instant. More details about this methodology can be found in Schmid and Brandt (2014).

2.4 Resolvent operator and input-output analysis

The resolvent operator relates the fluid system response to an external forcing. In this context, it is possible to investigate how a particular flow reacts to imposed disturbances, e.g. acoustic waves, heating, tripping, and vibrations, to name a few. To consider this input-output type of analysis, the linear system defined in the modal analysis (Eq. 7) is rewritten including an external forcing term $\mathbf{f}$. Following a state-space approach used in control theory, a supplementary equation is introduced to evaluate a user-specified output component $\mathbf{g}$ of the full state vector $\hat{\mathbf{q}}$ as

$$\begin{aligned} &\frac{\partial}{\partial t}\hat{\mathbf{q}} = \tilde{\mathbf{L}}\hat{\mathbf{q}} + \mathbf{B}\mathbf{f} \text{ , and} \\ &\mathbf{g} = \mathbf{C}\hat{\mathbf{q}} \text{ ,} \end{aligned} \tag{14}$$

where $\mathbf{B}$ and $\mathbf{C}$ determine the input and output quantities, respectively. The linear systems above can be solved as

$$\mathbf{g}(t) = \int_0^t \mathbf{C}\exp\left[(t-\tau)\mathbf{L}\right]\mathbf{B}\mathbf{f}(\tau)d\tau \text{ .} \tag{15}$$

This integral shows that the current output $\mathbf{g}$ depends on the entire forcing history $\mathbf{f}$. It is possible to solve the equation above numerically, but the intergral can be evaluated analytically if the external forcing is assumed to be harmonic, $\mathbf{f} = \hat{\mathbf{f}}\exp(i\omega t)$. Due to the linearity of the equations, the response is also harmonic under this assumption, $\mathbf{g} = \hat{\mathbf{g}}\exp(i\omega t)$. By substituting these assumptions into the integral, a simplified equation is obtained as

$$\hat{\mathbf{g}} = \mathbf{C}(i\omega\mathbf{I} - \tilde{\mathbf{L}})^{-1}\mathbf{B}\hat{\mathbf{f}} \text{ ,} \tag{16}$$

where $\mathbf{I}$ is the identity matrix. The equation above represents the system response due to the harmonic forcing.

To define the maximum energy gain of the system due to a harmonic forcing, the ratio between output and input is taken and maximized over all possible forcing profiles $\mathbf{f}$ for a given frequency ω, resulting in the resolvent norm represented as

$$R(\omega) = \max_{\hat{\mathbf{f}}} \frac{||\hat{\mathbf{g}}||_E^2}{||\hat{\mathbf{f}}||_E^2} = ||\mathbf{C}(i\omega\mathbf{I} - \tilde{\mathbf{L}})^{-1}\mathbf{B}||_E^2 = ||\mathbf{C}\mathbf{V}(i\omega\mathbf{I} - \mathbf{\Lambda})^{-1}\mathbf{V}^{-1}\mathbf{B}||_E^2 \text{ .} \tag{17}$$

The input-output analysis is performed by specifying the input and output of the resolvent norm by controlling the matrices $\mathbf{B}$ and $\mathbf{C}$. By solving both the resolvent operator and the input-output analysis through the application of a SVD, it is possible to obtain the optimal forcing and its respective response by looking at the left and right singular vectors associated with the dominant singular value.

3. RESULTS

This section presents results of modal and non-modal linear analyses of PRB flows. Initially the modal analysis is validated through a comparison of the eigenvalues for the plane Poiseuille flow followed by its comparison with the PRB setup. The non-modal analysis is validated through a comparison of transient growth results with John Soundar Jerome *et al.* (2012). As previously discussed, the discretization of wall-normal derivatives is performed using a fourth-order finite difference scheme, where 200 points are employed for all cases investigated in this work. A mesh refinement study showed that this resolution is sufficient to obtain convergence of results. Finally, the input-output analyses results are shown and the temperature influence is evaluated.

3.1 Validation of Results

For the modal analysis, the eigenvalues of the linear operator are first compared with those computed from Schmid and Henningson (2000) for the plane Poiseuille flow, as shown in Fig. (1a). Results are compared for the 20 most dynamically relevant eigenvalues for $Re = 2000$, $k = 1$ and $m = 0$. In the previous reference, the authors employ a spectral scheme to solve the Orr-Sommerfeld equation. Despite the differences in the numerical methodologies, excellent agreement is observed between the present results and those provided in the previous reference. Figure (1b) shows a comparison between a plane Poiseuille flow with $Re = 2000$ and a PRB flow with the same Reynolds number, besides $Ra = 1700$ and $Pr = 1$. It is possible to see that the unstable temperature gradient has little to no effect over the eigen-spectrum for this combination of k and m, which is expected since the Rayleigh-Bénard instabilities are more impactful for streamwise uniform disturbances ($k = 0$).

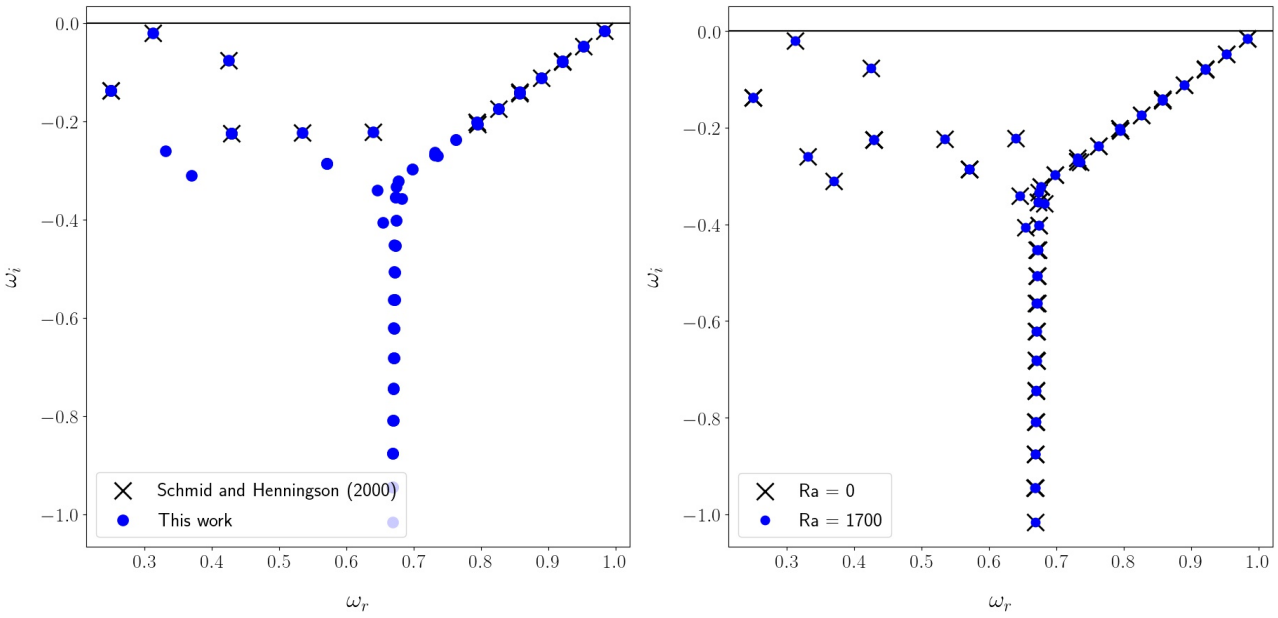

(a) Validation with Schmid and Henningson (2000) for $Ra = 0$ (b) Comparison for $Ra = 0$ and $Ra = 1700$

Figure 1: Eigen-spectrum of plane Poiseuille and PRB flows for $Re = 2000$, $Pr = 1$, $k = 1$ and $m = 0$.

For the non-modal analysis, a study of transient growth is performed for different Reynolds numbers and solutions are compared with those from John Soundar Jerome *et al.* (2012), for PRB flows. For all PRB cases investigated, the Rayleigh and Prandtl numbers are set as $Ra = 1500$ and $Pr = 1$, respectively. Two-dimensional streamwise disturbances are considered ($k = 0$) for a spanwise wavenumber $m = 2.04$. Figure (2) shows that the increase in the Reynolds number leads to a subsequent more pronounced increase in the energy of the system. However, the time for which the maximum transient growth is reached is approximately the same in non-dimensional units. One should also notice that, despite the curves for the lower Reynolds numbers reach higher maximum values in the plot, the growth rate is shown divided by the Reynolds number squared. Hence, it is clear that the $Re = 5000$ case has a higher amplification of disturbances.

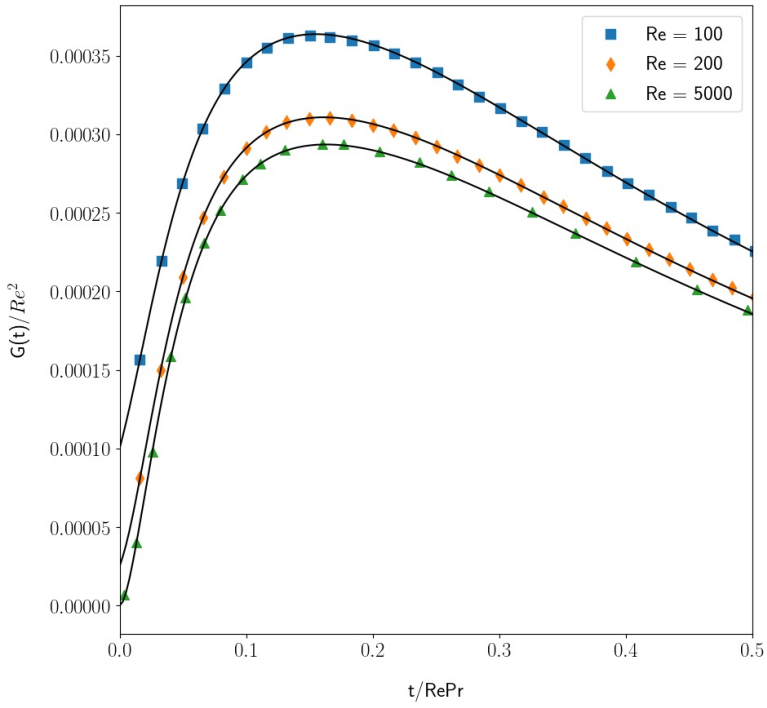

Figure 2: Transient growth for different Reynolds numbers and $Ra = 1500$, $Pr = 1$, $k = 0$ and $m = 2.04$. The continuous lines represent the present results while the symbols show results from John Soundar Jerome *et al.* (2012).

3.2 Input-Output Analysis

Two input-output analyses are performed in this section. The first is computed for the plane Poiseuille flow while the second is obtained for the PRB flow. Hence, it is possible to isolate the influence of the unstable temperature gradient on the analysis. Figures (3) and (4) are shown in log scale for the Poiseuille and PRB flows, respectively. These figures show how forcing in one flow variable, e.g. a velocity component, impacts the dynamics of some other variable.

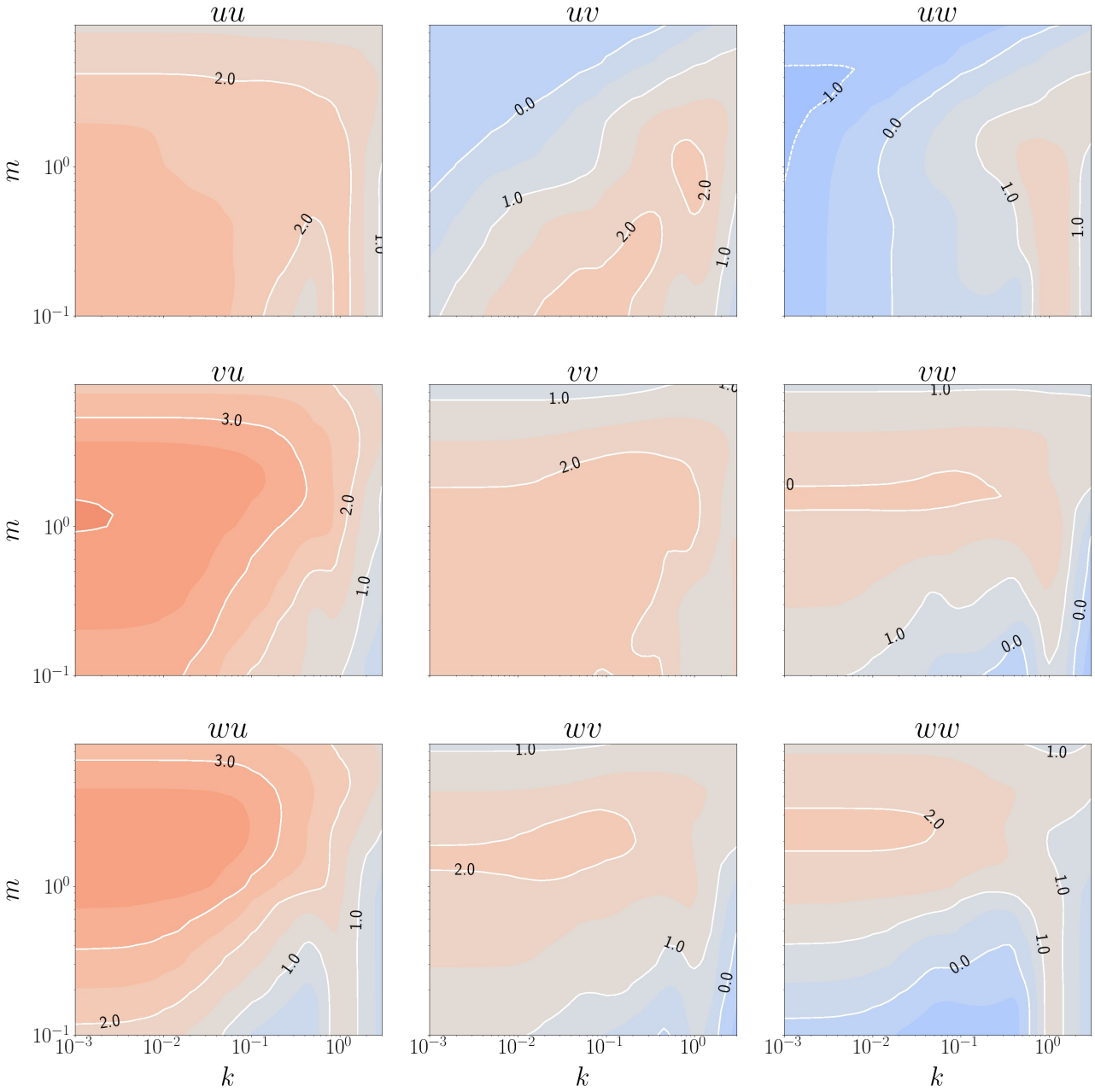

Figure 3: Input-output analysis for plane Poiseuille flow at $Re = 2000$ ($Ra = 0$, $Pr = 1$).

Figure 3 shows the input-output analysis for the plane Poiseuille flow. It is observed that the energy amplification is higher for input disturbances of velocity components v and w which lead to large responses in the u-velocity component. This shows that forcing the spanwise and wall-normal velocity components have a stronger influence on the flow response which has the highest impact on the streamwise velocity component. From the figure, the highest amplifications are observed for two-dimensional streamwise uniform modes. In a turbulent flow, for example, this would represent an energy transfer from the lift-up mechanism to form boundary layer streaks.

For the PRB flow, Fig. 4 shows that the highest energy transfer also occurs for the streamwise velocity component u. However, besides the velocity v and w inputs which are relevant in Poiseuille flow, for PRB flows, thermal inputs are also important. Comparing the present results to those from Fig. 3, the relevant amplification mechanisms remain the same,

with the addition of the temperature fluctuations. For the particular case studied in this work, the highest amplification in u is indeed observed for the temperature fluctuation input T since the Rayleigh number is almost at the instability limit. Despite this observation, one can also notice that the magnitudes of the other terms are also higher when compared to the plane Poiseuille case. Similarly to the Poiseuille flow, the highest amplification occurs for the streamwise uniform disturbance ($k = 0$).

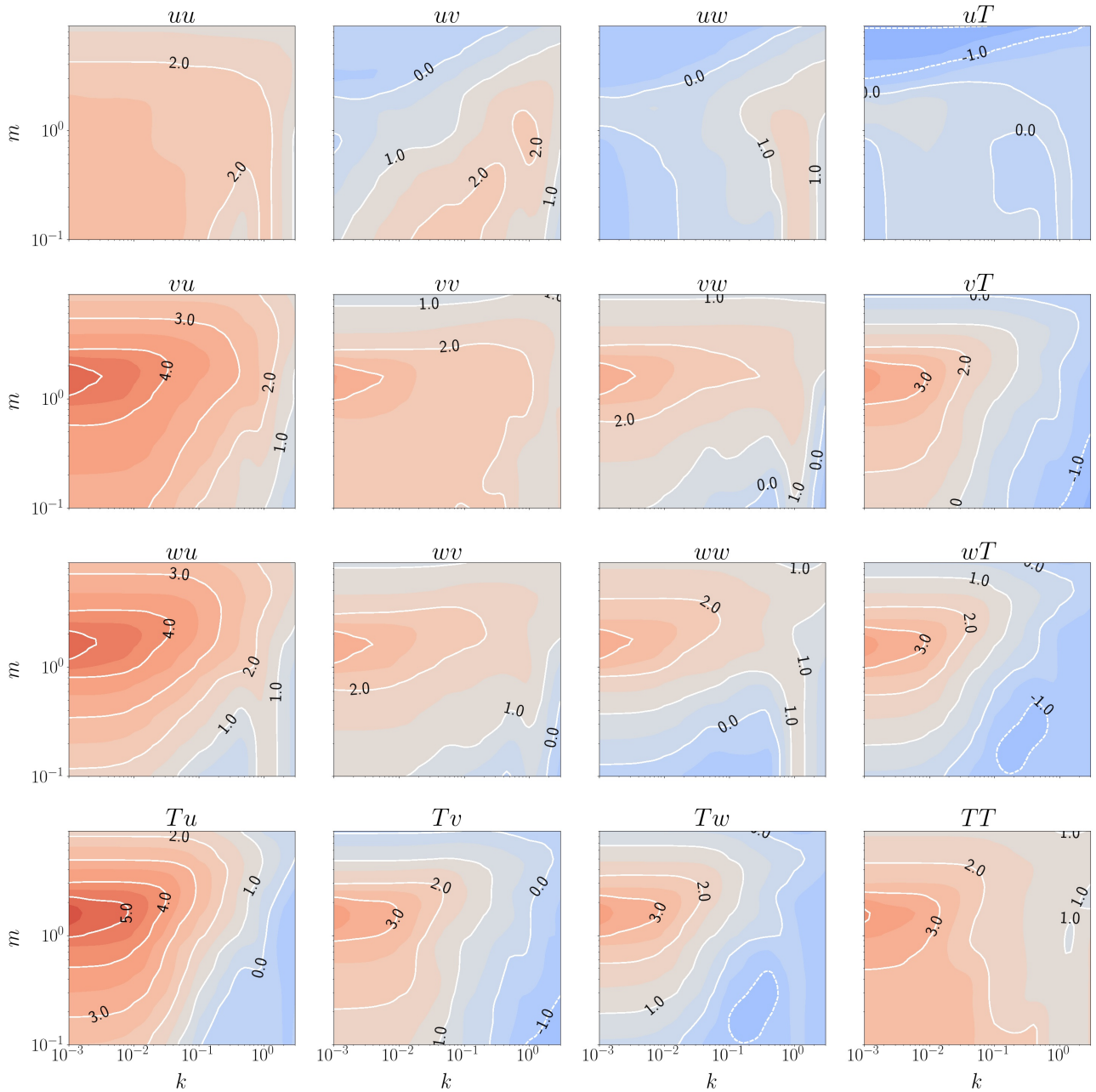

Figure 4: Input-Output Analysis for PRB flow at $Re = 2000$, $Ra = 1700$ and $Pr = 1$.

4. CONCLUSIONS

A temporal local stability analysis of a Poiseuille-Rayleigh-Bénard (PRB) flow is performed using modal and non-modal approaches. In order to first validate numerical results, the solution of the modal analysis is compared in terms of the eigen-spectrum for a plane Poiseuille flow. Then, results are computed for a PRB flow showing that the temperature gradient has little to no effect on the eigen-spectrum. Still, the thermal effects are largely noticed in a non-modal approach through the input-output analysis. In this case, forcing of temperature fluctuations is responsible for the highest responses in all other flow variables. It is also noticed that, although the thermal effects enhance the amplifications in the input-output analysis, they do not change the overall shape of the maps.

5. ACKNOWLEDGEMENTS

The authors acknowledge Fundação de Amparo à Pesquisa do Estado de São Paulo, FAPESP, for supporting the present work under research grant No. 2013/08293-7, and Conselho Nacional de Desenvolvimento Científico e Tecnológico, CNPq, for supporting this research under grants No. 407842/2018-7, 304335/2018-5 and 435413/2018-0. The first author is supported by a CNPq scholarship which is also acknowledged here.

6. REFERENCES

Chandrasekhar, S., 1961. *Hydrodynamic and hydromagnetic stability*. Oxford-Clarendon Press.

Idrac, P., 1920. "Sur les courants de convection atmosphérique et leur rapport avec le vol à voile et la formation des bandes nuageuses". *CRAS*, Vol. 171, pp. 42–44.

John Soundar Jerome, J., Chomaz, J.M. and Huerre, P., 2012. "Transient growth in Rayleigh-Bénard-Poiseuille/Couette convection". *Physics of Fluids*, Vol. 24, No. 4, p. 044103.

Jovanović, M.R. and Bamieh, B., 2005. "Componentwise energy amplification in channel flows". *Journal of Fluid Mechanics*, Vol. 534, pp. 145–183.

Nicolas, X., 2002. "Bibliographical review on the Poiseuille-Rayleigh-Bénard flows: the mixed convection flows in horizontal rectangular ducts heated from below". *International Journal of Thermal Sciences*, Vol. 41.

Nicolas, X., Luijkx, J.M. and Platten, J.K., 2000. "Linear stability of mixed convection flows in horizontal rectangular channels of finite transversal extension heated from below". *International journal of heat and mass transfer*, Vol. 43, No. 4, pp. 589–610.

Reddy, S.C. and Henningson, D.S., 1993. "Energy growth in viscous channel flows". *Journal of Fluid Mechanics*, Vol. 252, pp. 209–238.

Sameen, A. and Govindarajan, R., 2007. "The effect of wall heating on instability of channel flow". *Journal of Fluid Mechanics*, Vol. 577, pp. 417–442.

Schmid, P.J. and Brandt, L., 2014. "Analysis of fluid systems: Stability, receptivity, sensitivitylecture notes from the flow-nordita summer school on advanced instability methods for complex flows". *Applied Mechanics Reviews*, Vol. 66, No. 2.

Schmid, P.J. and Henningson, D.S., 2000. *Stability and Transition in Shear Flows*, Vol. 142. Springer Science & Business Media.

Trefethen, L.N., Trefethen, A.E., Reddy, S.C. and Driscoll, T.A., 1993. "Hydrodynamic stability without eigenvalues". *Science*, Vol. 261, No. 5121, pp. 578–584.

7. RESPONSIBILITY NOTICE

The authors are the only responsible for the material presented in this paper.